

Synthesis of the  $\text{Ca}^{2+}$ -mobilizing messengers, NAADP and cADPR, by intracellular CD38 enzyme in mouse heart: role in  $\beta$ -adrenoceptor signaling

Wee K. Lin<sup>1</sup>, Emma L. Bolton<sup>1</sup>, Wilian A. Cortopassi<sup>3,4</sup>, Yanwen Wang<sup>2</sup>, Fiona O'Brien<sup>1</sup>, Matylda Maciejewska<sup>1</sup>, Matthew P. Jacobson<sup>4</sup>, Clive Garnham<sup>1</sup>, Margarida Ruas<sup>1</sup>, John Parrington<sup>1</sup>, Ming Lei<sup>1</sup>, Rebecca Sitsapesan<sup>1</sup>, Antony Galione<sup>1</sup>, Derek A. Terrar<sup>1</sup>.

From the <sup>1</sup>Department of Pharmacology, University of Oxford, Mansfield Road, Oxford, OX1 3QT, UK

<sup>2</sup>Faculty of Biology, Medicine and Health, University of Manchester, Manchester, M13 9NT, UK

<sup>3</sup>Department of Chemistry, Chemistry Research Laboratory, University of Oxford, Mansfield Road, Oxford, OX1 3TA, UK

<sup>4</sup>Department of Pharmaceutical Chemistry, University of California, San Francisco, California 94158, United States

Running title: *Intracellular CD38 in heart and  $\beta$ -adrenoceptor signaling*

To whom correspondence should be addressed: Prof Derek A Terrar, Department of Pharmacology, University of Oxford, Mansfield Road, Oxford OX1 3QT, UK. Telephone: (+44) 1865271943; FAX: (+44) 1865271853; E-mail: derek.terrar@pharm.ox.ac.uk

**Keywords:**  $\text{Ca}^{2+}$ , beta-adrenoceptor, NAADP, cADPR, CD38, lysosomes, sarcoplasmic reticulum, heart, cardiac arrhythmia, cardiac hypertrophy

## ABSTRACT

Nicotinic acid adenine dinucleotide phosphate (NAADP) and cyclic ADP-ribose (cADPR) are  $\text{Ca}^{2+}$ -mobilizing messengers important for modulating cardiac excitation-contraction coupling and pathophysiology. CD38, which belongs to the ADP-ribosyl cyclase (ARC) family, catalyzes synthesis of both NAADP and cADPR *in vitro*. However, it remains unclear whether this is the main enzyme for their production under physiological conditions. Here, we show that membrane fractions from WT but not *CD38*<sup>-/-</sup> mouse hearts supported NAADP and cADPR synthesis. Membrane permeabilization of cardiac myocytes with saponin and/or Triton X-100 increased NAADP synthesis, indicating that intracellular CD38 contributes to NAADP production. The permeabilization also permitted immunostaining of CD38, with a striated pattern in WT myocytes, while *CD38*<sup>-/-</sup> myocytes and non-permeabilized WT myocytes showed little or no staining, without striation. A component of  $\beta$ -adrenoceptor signaling in the heart involves NAADP and lysosomes. Accordingly, in the presence of isoproterenol,  $\text{Ca}^{2+}$  transients and contraction ampli-

tudes were smaller in *CD38*<sup>-/-</sup> myocytes than WT. In addition, suppressing lysosomal function with bafilomycin A1 reduced the isoproterenol-induced increase in  $\text{Ca}^{2+}$  transients in cardiac myocytes from WT but not *CD38*<sup>-/-</sup> mice. Whole hearts isolated from *CD38*<sup>-/-</sup> mice and exposed to isoproterenol showed reduced arrhythmias. SAN4825, an ARC inhibitor, that reduced cADPR and NAADP synthesis in mouse membrane fractions, was shown to bind to CD38 in docking simulations, and reduced the isoproterenol-induced arrhythmias in WT hearts. These observations support generation of NAADP and cADPR by intracellular CD38, which contributes to effects of  $\beta$ -adrenoceptor stimulation (to increase both  $\text{Ca}^{2+}$  transients and the tendency to disturb heart rhythm).

ADP-ribosyl cyclases (ARC) are enzymes capable of converting nicotinamide adenine dinucleotide (NAD) into cyclic adenosine diphosphate ribose (cADPR). In addition, some of these cyclases, for example CD38 and Aplysia cyclase, can (at least under *in vitro* conditions) also produce nico-

nicotinic acid adenine dinucleotide phosphate (NAADP) using nicotinamide adenine dinucleotide phosphate (NADP) as substrate in the presence of nicotinic acid (NA) (see reviews in (1)). cADPR and NAADP are both potent  $\text{Ca}^{2+}$  releasing messengers (2, 3), which play significant roles in various signaling pathways in plants and animals, including humans (see reviews in (4, 5)). Cellular functions mediated by these two messengers include hormonal secretion, smooth muscle contraction, immune responses, fertilization and neuromodulation (4, 5). In the heart, both cADPR and NAADP modulate excitation-contraction coupling (6–9). These effects seem particularly important after stimulation of  $\beta$ -adrenoceptors, presumably associated with the elevated levels of NAADP and cADPR (7, 10, 11). It has been postulated that the increased concentrations of these messengers result from enhanced production by endogenous enzymes, and excessive production of these molecules contributes to the development of cardiac hypertrophy and arrhythmias associated with stimulation of  $\beta$ -adrenoceptors (9, 12, 13). The enzyme(s) responsible for the production of cADPR and NAADP is therefore a potential therapeutic target, and drugs including SAN4825 to target these enzyme(s) are under development (14). However, the nature and location of ARCs and/or NAADP-synthesizing enzymes in the heart remain unclear.

It was mentioned above that CD38 can function as an ARC catalyzing the synthesis of both cADPR and NAADP. However, a recent study on cardiac tissue suggests that CD38 mediates the synthesis of cADPR but not NAADP (15). This paper proposes that another cardiac enzyme on lysosomes synthesizes NAADP in response to intracellular  $\text{Ca}^{2+}$  fluxes in the myocyte following stimulation of  $\beta$ -adrenoceptors. The enzyme was referred to as NAADP-synthesizing enzyme (NSE). A further proposal was that NAADP produced within the lysosome causes  $\text{Ca}^{2+}$  release from this organelle, and this  $\text{Ca}^{2+}$  promotes cADPR synthesis by CD38 in neighboring endosomes. cADPR transported out of the endosome was then proposed to regulate ryanodine receptor opening in the sarcoplasmic reticulum (SR). Suppression of CD38 expression in  $\text{CD38}^{-/-}$  mice was shown to reduce the cardiac hypertrophy that is associated with chronic exposure

to the  $\beta$ -adrenoceptor agonist, isoproterenol (15). The proposal that CD38 promotes cADPR synthesis within the organelle is consistent with the commonly accepted view that CD38 can show activity as an ectoenzyme at the plasma membrane with an active site facing away from the cytosol (16). Work on lymphocytes first established the external orientation of CD38 (17). Since targets for NAADP and cADPR in cardiac muscle appear to be intracellular, the physiological relevance in the heart of enzyme activity of an ecto-CD38 remains unclear. Some have proposed expression of intraorganellar ARC (with an active site facing the lumen) in other tissues for cADPR and NAADP synthesis (see reviews in (18, 19)). Evidence from sea urchin egg supports the synthesis of cADPR within organelles followed by transport of the active substance into the cytosol to enable its participation in  $\text{Ca}^{2+}$  signaling (20). However, it has recently been suggested that CD38 can also exist in the opposite orientation with the active site of the enzyme facing the cytosol, and that the active site can still function to promote synthesis of cADPR in this topological orientation (21–23).

The aim of the present study was to further characterize the nature and identity of cADPR and NAADP-synthesizing enzymes in cardiac muscle, exploring their possible location on intracellular membranes and investigating the hypothesis that CD38 might function as the main enzyme responsible for the synthesis for both  $\text{Ca}^{2+}$  mobilizing messengers. The contributions of this pathway to physiological excitation-contraction coupling and pathological development of disturbances of cardiac rhythm were also investigated, since this pathway provides a novel target for development of anti-arrhythmic drugs.

## RESULTS

### *CD38 is the main enzyme responsible for cardiac synthesis of NAADP and cADPR*

A membrane-enriched preparation containing sarcolemma and SR was derived from mouse heart muscle both from WT and  $\text{CD38}^{-/-}$  mice. A sensitive bioassay for measuring NAADP was provided by sea urchin egg homogenates (SUEH) (24), which show a homologous desensitization of the  $\text{Ca}^{2+}$  releasing effect of NAADP at remarkably low concentrations (from approximately  $10^{-10}$  to

$10^{-8}$  M). Example traces and a calibration curve are shown in Fig 1A and Fig 1B. The membrane-enriched preparation from WT hearts produced NAADP when supplied with NADP and NA (Fig 1C and 1D). Interestingly, there was no comparable synthesis of NAADP with mixed membranes from  $CD38^{-/-}$  hearts ( $n = 3$ ;  $p \leq 0.001$ ; Fig 1C and 1D). A widely accepted conventional nicotinamide guanine dinucleotide (NGD) assay was used to determine the rate of cADPR synthesis (25). Using this assay, we detected the cyclization of NGD (an analogue of NAD) into cyclic GDP-ribose (cGDPR, a fluorescent analogue of cADPR) by membranes from WT hearts but not from  $CD38^{-/-}$  hearts ( $n = 6$ ;  $p \leq 0.001$ ; Fig 1E and 1F). These observations are consistent with the hypothesis that CD38 is the main enzyme responsible for the cardiac synthesis of both NAADP and cADPR.

#### ***Intracellular location of CD38 and possible association with SR***

Fig 2A shows that when the enzymatic activity of intact cardiac ventricular myocytes from WT mice was investigated using the same assay procedures as for the membrane enriched preparation from heart muscle above, there was very little synthesis of NAADP when cells were supplied with NADP and NA in the extracellular solution. However, permeabilization of the ventricular cell membranes with saponin (0.01% w/v) caused a substantial increase in the rate of production of NAADP consistent with access of substrates to the cell interior of healthy cells permitting production of NAADP by enzymes with intracellular active sites (Fig 2A). As saponin preferentially targets cholesterol-rich membranes (26) such as the sarcolemma rather than the SR, we then used Triton X-100 (0.1% v/v) to further expose potential intracellular enzymes (perhaps including those with lumen-facing active sites in various organelles). However, Triton X-100 permeabilization in the presence of saponin failed to cause a substantial increase the rate of NAADP production (Fig 2A). There appeared to be little or no difference between the effects of the two membrane permeabilizing agents applied alone or in combination (Fig 2B). The above experiments were repeated on intact myocytes from  $CD38^{-/-}$  hearts and there was little or no synthesis of NAADP both in intact myocytes and after membrane permeabilization with Triton

X-100 (Fig 2B). Control experiments showed that neither Triton X-100 nor saponin at the concentration used in these experiments affected the ability of the sea urchin egg homogenate bioassay to measure NAADP (Fig S1).

A rabbit polyclonal antibody to human CD38 was used to further investigate the presence of this enzyme in mouse ventricular myocytes, since the amino acid sequence (residue 1-170) used to generate the antibody showed extensive similarities between the two species (Fig S2). When the plasma membrane was intact in the absence of Triton X-100, there was little immunolabeling in WT mouse cardiac myocytes, and this labeling appeared to be concentrated in membrane patches (Fig 2C, top panels). When Triton X-100 was used to permeabilize the cell membrane, the labeling by the CD38 antibody was much more extensive and showed striations with a spacing corresponding to the sarcomere length of slightly less than  $2 \mu\text{m}$  (Fig 2C, middle panels). Convincing evidence that the human CD38 antibody was indeed labeling the mouse CD38 was provided by the observation that little or no labeling was detected in permeabilized cardiac ventricular myocytes from  $CD38^{-/-}$  mice (Fig 2C, bottom panels). This striated pattern with a spacing close to  $2 \mu\text{m}$  in myocytes from WT but not  $CD38^{-/-}$  mice is also supported by Fig 2D which shows plots of intensity for a line positioned along the long axis of the cell. Labeling by the antibody to human CD38 was also investigated in ventricular myocytes isolated from rabbit heart. In the presence of Triton X-100 to permeabilize cell membranes, immunolabeling with a striated pattern was again observed (Fig 2E) that appeared to be strikingly similar to that observed in WT mouse myocytes. Again the separation between striations appeared to correspond to sarcomere length, and labeling of ryanodine receptors (RyR2) showed a similar spacing. This immunolabeling with a striated pattern was not observed when Triton X-100 or primary antibody was omitted (Fig.2F). It therefore appears that membrane permeabilization was necessary for maximal NAADP synthesis and for labeling of intracellular CD38 in ventricular myocytes from WT mice, and that neither NAADP synthesis nor intracellular labeling of CD38 were observed in ventricular myocytes from  $CD38^{-/-}$  mice.

In addition, CD38 labeling on permeabi-

lized rabbit atrial myocytes was also found to have a striated pattern, similar to that observed in both mouse and rabbit ventricular myocytes (Fig S3). This observation provides support for association of CD38 with SR rather than t-tubules (see Discussion).

The observation that CD38 appears to be associated with the SR prompted us to investigate enzyme activity in a sheep SR vesicle preparation which is commonly used to investigate heart SR proteins including RyR2 (27–34). cGDPH synthesis with NGD as substrate was observed in this sheep cardiac SR preparation consistent with the presence of ARC activity (Fig S4A). As expected the effects were reduced in the presence of a CD38 inhibitor, nicotinamide (35). In Fig S4B, we show that isolated sheep cardiac SR vesicles were also able to synthesise NAADP when provided with NADP and NA. Both heavy (HSR) and light (LSR) SR fractions exhibited comparable NAADP synthesis (HSR:  $1.24 \pm 0.60 \text{ nmol mg}^{-1} \text{ min}^{-1}$ ; LSR:  $1.309 \pm 0.390 \text{ nmol mg}^{-1} \text{ min}^{-1}$ ;  $n = 4$ ;  $p = 0.9226$ ). This synthesis did not occur when sheep cardiac SR was provided with NADP alone, or NA alone (Fig S4C). This observation in sheep cardiac SR vesicles is consistent with our hypothesis of cardiac CD38 being expressed intracellularly and preferentially on the SR.

***The effects of isoproterenol to increase the amplitudes of  $\text{Ca}^{2+}$  transients (CaTs) and contractions accompanying electrical stimulation were smaller in cardiac myocytes from  $\text{CD38}^{-/-}$  mice than those in WT myocytes***

The functional effects of genetic knockout of CD38 were then investigated in cardiac ventricular myocytes. Previous work has shown that levels of NAADP and cADPR are elevated following  $\beta$ -adrenoceptor stimulation with isoproterenol (7, 11). It was also found that both NAADP and cADPR contribute, by different mechanisms, to the isoproterenol-induced increase in the amplitude of  $\text{Ca}^{2+}$  transients (CaTs) and contractions evoked by electrical stimulation in cardiac myocytes (7–9, 12). Consistent with these observations and the hypothesis that CD38 provides the major synthetic pathway for NAADP and cADPR, it was found that the amplitudes of CaTs and contractions in the presence of isoproterenol were smaller in cardiac myocytes from  $\text{CD38}^{-/-}$  mice than in myocytes from WT mice (Fig 3A - D).

***Bafilomycin A1, to inhibit lysosomal-NAADP function, reduced the increase in amplitude of CaTs caused by isoproterenol in electrically stimulated myocytes from WT but not  $\text{CD38}^{-/-}$  mice***

In the case of NAADP actions, previous work has demonstrated that a component of the isoproterenol-induced increase in the amplitude of CaTs induced by electrical stimulation appears to depend on NAADP acting via TPC2 channels in lysosomal membranes (9). Lysosomes have also been shown to form associations with the SR consistent with the formation of  $\text{Ca}^{2+}$  microdomains between the organellar membranes (36). In addition, it has been shown that when lysosomal-NAADP function is disrupted with bafilomycin A1 the increase in CaT amplitude caused by isoproterenol is reduced (7, 9). The reduction in the isoproterenol-induced increase in the amplitude of CaT following bafilomycin A1 treatment ( $10 \mu\text{M}$ ) is shown again here for WT myocytes, but in contrast bafilomycin A1 failed to reduce the isoproterenol-induced increase in CaT amplitude in myocytes from  $\text{CD38}^{-/-}$  mice (Figure 3E). This was also evident from the ratio of effects of isoproterenol with and without bafilomycin A1 in Fig 3F (showing lack of difference in  $\text{CD38}^{-/-}$  myocytes compared with reduced effect in WT). Sample records are shown in Fig 3G. These observations are therefore consistent with the hypothesis that cardiac myocytes from  $\text{CD38}^{-/-}$  mice are unable to synthesize significant amounts of NAADP, and therefore this pathway can no longer be functionally suppressed by bafilomycin A1. The observations therefore provide further support for a role for NAADP synthesized by CD38 in this physiological process in WT cardiac muscle. The remaining isoproterenol-induced increases in myocytes from  $\text{CD38}^{-/-}$  mice are likely to have resulted at least in part from the expected PKA mediated effects on L-type  $\text{Ca}^{2+}$  channels and phospholamban that are thought not to involve CD38 (37). The CD38-dependent pathway underlying these observations is considered at greater length in the Discussion.

***In vitro and in silico evidence showed that a novel inhibitor of cardiac ARC, SAN4825, also inhibited NAADP synthesis at physiological pH, possibly through targeting CD38***

SAN4825 is a novel drug developed as an



inhibitor of cardiac specific ARCs, and has been shown (14) to suppress the ability of a rat SR membrane preparation to synthesize a fluorescent analogue of cADPR ( $IC_{50} \approx 1.3 \mu M$ ). This drug was also shown to partially inhibit the ARC activity of human purified CD38 at higher concentration (14). We tested for the ability of SAN4825 to inhibit both NAADP and cADPR synthesis by the mouse membrane preparation for which the evidence reported above shows CD38 to be the major enzyme catalyzing synthesis of these  $Ca^{2+}$ -mobilizing messengers. SAN4825 was observed to cause a concentration-dependent inhibition of both NAADP synthesis (Fig 4A) and cADPR synthesis (Fig 4B). Similar inhibition of NAADP synthesis by SAN4825 was also observed in saponin-permeabilized myocytes from mouse hearts (Figure S5). SAN4825 inhibition of NAADP synthesis was observed to be greater at pH 7.2 and this will be considered at greater length in Discussion.

The active site residues Glu150, Asp159, Glu230, Trp129 and Trp193 in mouse CD38 correspond to Glu146, Glu226, Asp155, Trp125 and Trp189 in human CD38. These residues in human CD38 are believed to play an important role for NAADP and cADPR synthesis following mutagenesis studies (38). In a docking simulation using Glide, we demonstrate that the most favorable docking conformation of SAN4825 at pH 7.2 in mouse CD38 (PDB ID: 2EG9 (39)) is in close proximity to these active site residues (Fig 4C). Further superimposition of the binding conformation of SAN4825 in mouse CD38 with the binding conformations of an NAADP analogue and ADPRP in human CD38 (PDB ID: 4F46 (40)) suggests that SAN4825 occupies the same binding site as these substrates, in close proximity to Glu230 of mouse CD38 (Fig 4C). The pyridine ring of SAN4825 also showed  $\pi$ - $\pi$  stacking with Trp193 of mouse CD38. These  $\pi$ - $\pi$  interactions were also observed in the crystal structure of wild type human CD38 in complex with the NAADP analogue and ADPRP (40).

Further computational studies also demonstrated that the single active site is the only plausible binding site of SAN4825. Specifically, blind docking results using SwissDock showed that approximately 90% of the predicted docking sites (250 predictions in total) of SAN4825 in mouse CD38

are within 4.5 Å from the centre of the active site (Figure 4D and E). SiteMap also presented a similar result, showing that the active site is the only site to present a SiteScore value closer to 1.0 (0.97), indicative of a difficult, but druggable site, with an estimated volume of 286 Å<sup>3</sup>. The other binding sites presented SiteScore values close to 0.8, suggestive of undruggable cavities, with volumes smaller than 120 Å<sup>3</sup>. Taken together, these observations suggest that SAN4825 acts as a competitive inhibitor of NAADP and cADPR synthesis.

#### ***CD38<sup>-/-</sup> hearts were more resistant to arrhythmias during over-stimulation of $\beta$ -adrenoceptor pathway.***

It is known that excessive  $\beta$ -adrenoceptor stimulation can lead to cardiac arrhythmias (41). The tendency to arrhythmias in intact mouse hearts was assessed by four different protocols (burst pacing with increasing frequency, 50 Hz burst pacing with increasing current, S1S2 pacing and dynamic pacing; see Experimental Procedures for details and scoring methods). WT hearts showed a significant increase in arrhythmogenicity after application of 300 nM isoproterenol (Fig 5A). In contrast, no significant increase in arrhythmogenicity was observed following isoproterenol application in hearts from the *CD38<sup>-/-</sup>* mice (Fig 5A). Two other methods of presentation of the data were used to highlight changes in arrhythmogenicity. Fig 5B shows the increase in arrhythmogenic events after isoproterenol, and demonstrates the significant reduction in arrhythmogenicity in hearts from the *CD38<sup>-/-</sup>* mice as compared with WT. When the observations were plotted as pie charts representing the proportion of hearts showing arrhythmias, it was clear that the proportion of hearts from *CD38<sup>-/-</sup>* mice that were susceptible to isoproterenol-induced arrhythmogenicity (one of six hearts) was less than the corresponding proportion of WT hearts (seven of eight hearts, Fig 5C).

The cumulative percentage of hearts which became arrhythmic in the presence of isoproterenol (300 nM) during the burst pacing protocol with increasing pacing frequency and increasing pacing current is shown in Fig 5D, once again showing that hearts from *CD38<sup>-/-</sup>* mice had a reduced tendency to arrhythmias under these conditions. Hearts from WT mice also had a significantly lower current

threshold for initiation of arrhythmias, as shown in Fig 5E. Percentages of  $CD38^{-/-}$  hearts that exhibited sign of arrhythmias (in the absence and presence of 300 nM isoprenaline) during dynamic pacing and S1S2 pacing protocols was also lower than those of WT hearts (Fig 5F). Representative traces are shown in Fig 5G. Taken together these observations show that the tendency for arrhythmias during exposure to high concentrations of  $\beta$ -adrenoceptor agonist was greatly reduced in hearts from  $CD38^{-/-}$  mice.

Having shown that 3  $\mu$ M SAN4825 is sufficient to inhibit the production of NAADP and cADPR synthesis, we further investigated its anti-arrhythmogenic effect. The effects of 3  $\mu$ M SAN4825 on the tendency for arrhythmias during excessive  $\beta$ -adrenoceptor stimulation were broadly similar to the consequences of genetic knockdown of CD38 described above (Fig 5A-G), although the drug effects appeared to be less than CD38 knockout.

## DISCUSSION

The main findings reported here are that CD38 is the principal enzyme in heart muscle responsible for synthesis of two  $Ca^{2+}$ -mobilizing messengers NAADP and cADPR, and that a major component of CD38 appears to be intracellular, perhaps associated with the SR (although there may be some additional CD38 enzyme on the cell surface). These findings are consistent with the conclusions of Gul et al that CD38 mediates synthesis of cADPR in cardiac myocytes, but contrast with Gul et al in their proposal that a different enzyme (NSE), is responsible for NAADP production in these cells (15).

In comparing our observations with those of Gul et al (15), it is important to note differences in the experimental conditions, particularly with respect to the actions of isoproterenol. In our experiments effects of  $\beta$ -adrenoceptor stimulation were studied in a physiological condition where cardiac myocytes were paced and the amplitude of CaTs triggered by electrical stimulation were investigated at low concentrations of isoproterenol (2 to 5 nM). In contrast, the increases in cytosolic  $Ca^{2+}$  reported by Gul et al were in cardiac myocytes that were not electrically paced and for which the isoproterenol concentration was 1000 times greater (2  $\mu$ M) (15). These very high concentrations of isoproterenol are likely to have caused spontaneous  $Ca^{2+}$  waves and/or os-

cillations, and the recorded maintained increases in cytosolic  $Ca^{2+}$  may have been the result of summation of signals (with an image collection rate of one per 3s) from many cardiac myocytes in the field of view.

Gul et al have suggested that NAADP production precedes synthesis of cADPR and propose that  $Ca^{2+}$  released from lysosomes by NAADP reaches nearby CD38 in endosomes causing an increase in the enzyme activity of CD38 to produce cADPR (15). This interpretation relies on observations in their Fig 2, although it could be argued that the quite small observed differences in apparent time to peak synthesis of NAADP or cADPR (that appeared to be 15 s, or one measurement time point) may result from the ability to detect these messengers rather than reflect differences in the underlying physiology. Previous work in whole hearts shows that production of both cADPR and NAADP occurs rapidly following isoproterenol addition (11). It should also be mentioned that protein structural work shows that binding of  $Ca^{2+}$  causes conformational changes in CD38 that are expected to be inhibitory rather stimulatory for enzyme action, while functional studies show little or no change in enzyme activity at the  $Ca^{2+}$  concentrations likely to be experienced by intracellular CD38 (42).

The possibility that the major active enzyme, CD38 is located at or close to SR membranes is supported by our immunohistochemical observations showing CD38 labeling has a striated pattern with a spacing that closely resembles that of the SR protein, RyR2, both in ventricular and atrial myocytes. The lack of similar immunohistochemical staining in myocytes from  $CD38^{-/-}$  mice demonstrates that these observations are unlikely to result from lack of specificity of the antibody used to identify CD38. Since atrial myocytes lack the extensive t-tubule network seen in ventricular myocytes (and atrial t-tubules do not show the regular sarcomere spacing observed in ventricle), the striated pattern also seen in atrial myocytes must result from staining of CD38 that appears to be associated with the SR (which does show a striated pattern in both atrial and ventricular muscle). It has recently been shown that lysosomes also show some association with the SR (as well as mitochondria) but the striated pattern for lysosomal markers is less distinct than the

observations reported here for CD38 (36).

Although evidence for NAADP and cADPR function in cardiac myocytes has so far been demonstrated only in mouse, rat and guinea-pig (7–10, 43, 44) it is our hypothesis that this pathway operates in all mammalian hearts, and that CD38 associated with the SR is the main synthetic enzyme. In the past, SR membrane preparations from the hearts of various animals have been used as a model to study the synthesis of cADPR or cGDPR by ARC (10, 14, 45, 46). In particular, sheep SR preparations have been widely used for the study of RyR2 and other SR proteins (27–34). We are the first to show that in addition to catalysis of the cyclization reactions, sheep SR vesicles can also catalyze the base exchange reaction that produces NAADP (Fig S4). Although functional effects of this pathway have yet to be investigated in sheep, this species has the advantage of allowing easy preparation of amounts of biological material that are orders of magnitude greater than can be prepared from much smaller mouse hearts. The relative purity of similar preparations is supported by electron microscopy and biochemical studies (45, 47, 48). Most importantly, to date, CD38 is the only mammalian enzyme that has been identified with the ability to synthesize both cADPR and NAADP, as a consequence of reactions at a multifunctional active site (see reviews (49)). Although we are yet to fully characterize the ARC on sheep SR, our initial investigations show that the enzymatic properties observed in sheep SR preparations have a high resemblance to those of human and mouse CD38. Therefore, our observations on sheep SR vesicles corroborate our hypothesis that CD38 is expressed intracellularly and appears to show a preferential association with the SR in cardiac tissue.

The functional observations with the Sanofi drug, SAN4825, which reduced synthesis of both NAADP and cADPR, are consistent with its inhibitory actions at a single enzyme. The most favorable Glide docking conformations of SAN4825 with mouse CD38 at pH 7.2 suggest that this compound occupies the same binding site as the NAADP analogue and ADPRP, in close proximity with Glu226. The pyridine ring of SAN4825 also shows  $\pi$ - $\pi$  interaction with the Trp189 of mouse CD38. The blind docking results from the Swissdock server

also predicted a single inhibitory binding site for the SAN4825, and this site corresponds to the enzymatic active site of CD38. These SAN4825-CD38 binding conformations showed some resemblance to the native binding conformation between CD38 and its substrates, such as NAD, NMN, cADPR and NAADP (40, 50, 51).

Interestingly, the inhibition of NAADP but not cADPR synthesis by SAN4825 was observed to be greater at the cytosolic pH of 7.2 than at the acidic pH of 4.5 (Fig 4A, B). Therefore, we further investigated the binding conformations of SAN4825 at the active site of mouse CD38 with considerations of different protonation states of SAN4825 and mouse CD38 protein amino acids predicted by Epik and Propka 3.1, respectively (Fig S6). The SAN4825 molecule can be protonated or unprotonated, and CD38 will adopt different protein conformations at different pH values. Nevertheless, with all four combinations (two SAN4825 protonation states and two CD38 conformations), all the predicted binding sites of SAN4825 were still in proximity of the catalytic residues of mouse CD38 (Fig S6). In considering the weakening of inhibition of NAADP synthesis by SAN4825 at pH 4.5, the following factors need to be taken into account: i) NAADP synthesis by human CD38 (3) and mouse CD38 (Fig 4A) was observed to be enhanced at pH 4.5; ii) inhibition of cADPR synthesis by SAN4825 remained unchanged at pH 4.5 (Fig 4B); iii) SAN4825 was predicted to bind to the CD38 active site at both pH 7.2 and pH 4.5 (Fig S6); iv) no NAADP synthesis was observed in membrane fractions from *CD38*<sup>-/-</sup> mice at pH 4.5 (Fig S7); in view of these observations and predictions, it appears that the observed weakened inhibition of SAN4825 at pH 4.5 does not result from a degradation of the drug, or from a major change in the binding conformation of the drug, and cannot be accounted for by a non-CD38 enzyme synthesizing NAADP. Although a weakened inhibition of NAADP synthesis by SAN4825 was observed at pH 4.5, evidence from our docking simulations and *in vitro* experiments still supports the ability of SAN4825 to inhibit the synthesis of NAADP and cADPR as a competitive inhibitor.

What are the implications of our findings for the normal physiology of the heart? Our observations show that the amplitudes of CaTs initiated

by electrical stimulation at a constant rate were increased by  $\beta$ -adrenoceptor stimulation with isoproterenol at low concentrations (2 to 5 nM) and that part of this response was prevented in WT mice by the use of bafilomycin A1 to suppress the contribution of the lysosomal pathway involving NAADP and TPC2 (9). In contrast, myocytes from  $CD38^{-/-}$  mice bafilomycin A1 no longer suppressed this component of the isoproterenol action, consistent with importance of CD38 in the mechanism underlying NAADP production and subsequent response. This is consistent with the need for coupling of CD38 to receptors, leading to NAADP synthesis and action via TPC2 proteins in the cardiac lysosomal signaling pathway (7, 44).

Previous experiments support elevation of NAADP and cADPR levels in response to  $\beta$ -adrenoceptor stimulation by isoproterenol (7, 10, 11, 52). Our observations show that genetic knock out and pharmacological inhibition of CD38 provide resistance for arrhythmias associated with acute exposure to excessive stimulation  $\beta$ -adrenoceptors compared with WT hearts. Taken together these observations are consistent with an effect of  $\beta$ -adrenoceptor stimulation by as yet unidentified mechanisms to enhance the catalytic activity of CD38 leading to increased levels of these  $Ca^{2+}$  mobilizing messengers (7, 11) which in turn enhance CaTs evoked by cardiac action potentials or trigger arrhythmic events resulting from excessive  $Ca^{2+}$  mobilizing messengers.

We have recently shown that the cardiac hypertrophy and associated tendency to arrhythmias that is provoked by chronic exposure to  $\beta$ -adrenoceptor stimulation is markedly reduced when the influence of the NAADP pathway is suppressed in mice lacking NAADP-regulated TPC2 proteins (9). Since CD38 is upstream in this signaling pathway it seems reasonable to propose that CD38 contributes to these processes and that hearts from  $CD38^{-/-}$  mice might also be resistant to cardiac hypertrophy and associated arrhythmias following chronic exposure to  $\beta$ -adrenoceptor stimulation. The recent observations from Gul et al show that this is indeed the case and provide further support for this hypothesis (15).

Graeff et al have suggested that a protonation of NA at acidic pH is essential for the binding

of NA to acidic residues (Glu146 and Asp155) on CD38, because at neutral pH the electrostatic repulsion between them would reduce substrate binding and consequently the rate of NAADP synthesis (53). However, our observations showed that cardiac muscle CD38 can catalyze the formation of NAADP at physiological pH, although at a lower rate than at acidic pH. It should also be noted that as a result of the remarkably high potency of NAADP as a  $Ca^{2+}$  releasing messenger, the threshold concentration for NAADP to cause lysosomal  $Ca^{2+}$  release is very low, probably in the tens of nM range (7), and therefore even a small amount of synthesized NAADP at pH 7.2 would be enough to activate the NAADP signaling pathway. This hypothesis is further supported by the work of HC Lee and colleagues demonstrating that the active site of CD38 can remain functional under the reducing conditions of the cytosol and at cytosolic pH (23).

Although CD38 was thought to exist as type II transmembrane protein with its C-terminal catalytic domain on the outside of the cell, Zhao et al. showed in cell lines and primary human cells the presence of a proportion of CD38 in the type III form, with the catalytic domain facing the cytosol (22). In our study, substrates to permit synthesis of NAADP and/or cADPR were not included in the perfusion solution for intact heart or single cell studies, and even if there were extracellular synthesis of these messengers it seems likely that any relevant transporter of molecules will be made redundant or inefficient as a consequence of the constant flow of perfusion solution under the conditions of our experiments. These factors are expected to prevent the cytosolic accumulation of NAADP and cADPR from an extracellular source, and we have therefore favored arguments that in cardiac cells, CD38 in the type III form might mediate intracellular synthesis of these  $Ca^{2+}$  mobilizing agents in WT type animals leading to the observed effects on CaTs, contraction and arrhythmogenicity of the heart. This is consistent with our observations that permeabilized single cells (using saponin and/ or Triton X-100) have higher enzymatic activity. Permeabilization was also required for immunolabeling of CD38. The finding that a functionally important component of CD38 appears to be intracellular and associated with the SR in heart should not be thought to be in conflict



with observations showing other locations for similar enzymes in different cell types (16, 19, 20, 54). It is possible that the  $\text{Ca}^{2+}$  signaling molecules cADPR and NAADP are so important in many diverse roles in the plant and animal kingdoms that different locations of synthetic enzymes may have evolved to suit different functional needs.

Since the known major modulatory influences of NAADP and cADPR on CaTs in cardiac myocytes have been shown to be mediated through SR-associated proteins (sarco-endoplasmic reticulum  $\text{Ca}^{2+}$ -ATPase and RyRs) (9, 43, 55), it seems reasonable to propose that the most efficient operation of the signaling pathways involving NAADP and cADPR might be best served by a CD38 synthetic enzyme that is predominantly intracellular (perhaps located at or close to the SR membrane). An interesting hypothesis would be that CD38, NAADP and cADPR, as well as the relevant substrates could act within microdomains close to sites of  $\text{Ca}^{2+}$  uptake and/or release on the SR membrane, thereby facilitating the signaling pathways (see Scheme in (44)). Our recent observations concerning the location of lysosomes in close proximity to SR is relevant in this context (36).

In the above discussion, the main focus is to highlight the pivotal role of intracellular CD38 in catalyzing the cyclization and base exchange reactions in hearts, particularly following activation of the  $\beta$ -adrenoceptor pathway. There are several limitations to this study. Although we have proposed that the CD38 enzyme appears to be associated with SR membranes, we have not addressed the topology of the enzyme, particularly concerning the orientation of the active site, and this will be the subject of future experiments. In addition although this study adds to previous work showing a link between  $\beta$ -adrenoceptor stimulation and synthesis of NAADP and cADPR, further work is needed to establish the extent of activation of the CD38 pathway in the absence of this stimulation, and to investigate the cellular mechanisms by which  $\beta$ -adrenoceptor stimulation upregulates CD38 activity.

In conclusion, this study provides novel evidence for cardiac synthesis of two potent and important  $\text{Ca}^{2+}$  mobilizing molecules, NAADP and cADPR, by intracellular CD38, probably associated with or close to the sarcoplasmic reticulum. The

cellular pathway starting with CD38 and involving NAADP and cADPR acts to enhance excitation-contraction coupling particularly during activation of  $\beta$ -adrenoceptors. Our observations demonstrating that  $\text{CD38}^{-/-}$  hearts are resistant to  $\beta$ -adrenoceptor-associated arrhythmias also reveal the potential of targeting CD38-signaling pathways to treat cardiac disease.

## EXPERIMENTAL PROCEDURES

### *Single cell studies*

**Cell isolation** – The  $\text{CD38}^{-/-}$  mouse line was developed by Cockayne et al (56) and obtained from Jackson laboratory ( $\text{Cd38}^{\text{tm1Lnd}}/\text{J}$ ). The protocol for generating and maintaining the mice was approved by the Oxford University Ethical Review Committee (Pharmacology subcommittee) and Home Office. We confirm that all methods were performed in accordance with the relevant UK Home Office and institutional guidelines and regulations. Ventricular myocytes were isolated from male mice (C57BL6 or  $\text{CD38}^{-/-}$ , 16 – 24 week-old) and male New Zealand White rabbits (approximately 1 kg) using 0.3-0.5 mg  $\text{mL}^{-1}$  collagenase (type II, Worthington Biochemical Corp., NJ, U.S.A.) The detailed methods were described in (9, 36). Rabbit atrial myocytes were isolated using a similar protocol to that used to isolate rabbit ventricular myocytes

**$\text{Ca}^{2+}$  imaging in single cardiac myocytes** – Mouse myocytes were incubated with fluo-5F AM (5  $\mu\text{M}$ ) for 20 min. CaTs were stimulated at 1 Hz by carbon-fibre electrodes placed at the side of the superfusion bath. Mouse ventricular myocytes were visualised using a Nikon Axiovert 200 inverted microscope with attached Nipkow spinning disk confocal unit (CSU-10, Andor Technology, UK). Excitation light was provided by a 488 nm diode laser (Cairn Research Ltd, Kent, UK) passed through the Nipkow unit and delivered to the sample through the objective. Emitted light passed back through the CSU-10 unit and was detected using an Andor iXON897 EM-CCD camera (Andor Technology, UK) at a 50 frames per second. Images were recorded and analyzed using Andor iQ software (Andor Technology, UK). For analysis, background fluorescence was subtracted and multiple transients were averaged to obtain the basal CaTs before isoproterenol application and the peak CaTs amplitude during 5

min isoproterenol application. Data are presented as  $F/F_0$  such that fluorescence data are presented relative to diastolic fluorescence.

**Contraction studies** – Cells were stimulated at 1 Hz by carbon-fibre electrodes placed at the side of the superfusion bath and contractile properties studied using the IonOptix system (IonOptix Corp., MA, USA) to measure sarcomere length. Cells were visualised via a 40x oil objective using an IonOptix MyoCam (IonOptix Corp.) which sampled images at a frequency of 240 Hz. Sinusoidal optical density traces arising from the alternating light and dark bands of the contractile machinery were then transformed into a signal of sarcomere length by application of a fast Fourier transform (FFT) by the IonWizard sarcomere length acquisition software (IonOptix Corp.). Length measurements were calibrated using a stage micrometer with 2  $\mu$ m graduations such that the number of pixels per  $\mu$ m recorded by the MyoCam could be entered into the software as a fixed value. Amplitude of sarcomere shortening was calculated by deduction of systolic from diastolic sarcomere length. Analysis was performed using IonWizard 5 software (IonOptix Corp.). All values represent an average of 10 contractions.

Cell for both  $Ca^{2+}$  imaging experiments and contraction studies were superfused with medium containing (mM): NaCl 130, KCl 5.4,  $MgCl_2$  3.5,  $CaCl_2$  1.8 glucose 10, HEPES 5,  $NaH_2PO_4$  0.4, pH 7.4; 36 °C.

### ***In vitro biochemical assay***

**Mixed membrane and sarcoplasmic reticulum-enriched membrane preparations**—As previously described, mixed membrane vesicles were prepared from sheep (obtained from an abattoir) or mouse male mouse (C57BL6 or  $CD38^{-/-}$ , 12-20 week old) cardiac tissue (57) A discontinuous sucrose gradient was used to separate the sarcolemmal membrane from the light SR (LSR) and heavy SR (HSR) membrane fractions. For each tissue, the protein concentration was calculated using a Bradford assay (58) and the various membrane fractions were aliquoted and stored at -80 °C.

**Assessment of the enzymatic cyclisation rate of ADP-ribosyl cyclase** – A final concentration of 500  $\mu$ M NGD was added to the protein sample to initiate the enzymatic reaction. The cGDPR formation was monitored through its fluorescence intensity at 410

$\pm$  5 nm during excitation with light of wavelength  $300 \pm 3$  nm (25). The cyclase activity of each reaction mixture was then defined by the change in fluorescence with time, i.e., the slope of the line in the fluorescence versus time plot obtained by linear regression.

**Detection and quantification of NAADP production**—The level of NAADP production was quantified by the means of NAADP inactivation bioassay using sea-urchin egg homogenates (SUEH) (24). The SUEH were prepared using the method reported (59). Free  $Ca^{2+}$  concentration was measured with fluo-3 by monitoring fluorescence intensity at excitation and emission wavelengths of 490 and 535 nm, respectively.. To synthesize NAADP, 500  $\mu$ M NADP and 7 mM NA were preincubated with the SR-enriched cardiac preparation at 37 °C. Then, the protein-substrate mixtures were diluted before adding to the sea-urchin egg homogenate. After 5 min, a standard 500 nM purified NAADP was further added to the sea-urchin egg homogenate to elicit a submaximal NAADP-induced  $Ca^{2+}$  release. The  $Ca^{2+}$  release response to the standard 500 nM NAADP is dependent on the subthreshold concentration of the NAADP in the preceding protein-substrate mixture addition. The concentration of NAADP in the protein-substrate mixture were quantified through interpolation of a standard dose response curve from known concentrations of purified NAADP.

For both NGD and SUEH assay, 10-20  $\mu$ L of the SR-enriched or mixed membrane cardiac preparation was incubated in a solution containing (mM): KCL 150,  $MgCl_2$  0.5 and HEPES 10; pH 7.2. An acetate-based buffer was used in the condition where an acidic pH of 4.5 is required. For experiments investigating the enzymatic activities of permeabilised myocytes, myocytes were incubated with solution comprising of (mM): KCl 70,  $MgCl_2$  5, K glutamine 5, taurine 20, EGTA, 0.04, succinic acid 5,  $KH_2PO_4$  20, glucose 10, HEPES 5, pH 7.2 with KOH. This solution is spiked with either saponin 0.01 % w/v. or Triton X-100 0.1 % v/v. Fluorimetry was performed in a Novostar plate reader (BMG Labtech).

### ***Immunocytochemistry studies***

Cells were fixed in in 4% paraformaldehyde/PBS for 15 min, washed in PBS (3 changes, 5 min each), permeabilized using 0.1% Triton X-100 (Sigma-

Aldrich) for 10 min, washed in PBS, blocked with 1 % bovine serum albumin for 60 min before being incubated with the primary antibody at 4 °C overnight. The next day, cells were first washed with PBS before being incubated with secondary antibody at RT for 2 hours (either AlexaFluor 488 conjugated donkey anti-rabbit or Dylight 550 donkey anti-mouse, 1: 1000 dilution) then washed. Finally, coverslips were mounted using Vectashield® and permanently sealed. Cells were stored in the dark at 4°C and visualized within 2 days. For control experiments, we performed the same procedure with the omission of the primary antibodies or with cells from *CD38*<sup>-/-</sup> mice. Primary antibodies against CD38 (sc-15362, Santa Cruz) and RyR2 (ab2827, Abcam) were used at a 1 : 100 and 1 : 200 dilution respectively. Observations were carried out using a Nikon A1 confocal laser scanning microscope equipped with a 60x objective, and images were processed using ImageJ software.

#### ***Ex-Vivo programmed electrical stimulations (PES)***

Hearts were isolated from male mice (16-24 week-old) and mounted in a Langendorff perfusion system. Hearts were perfused with Krebs solution comprising of (mM): NaCl 119, NaHCO<sub>3</sub> 25, KCl 4, Na pyruvate 1.8, KH<sub>2</sub>PO<sub>4</sub> 1.2, MgCl<sub>2</sub> 1, CaCl<sub>2</sub> 1.8, glucose 10 (pH 7.4) 37 °C. Hearts were left to stabilise for 30 mins. During this 30 mins time window, hearts were also preincubated with drugs or vehicle present inside the Krebs solutions. To assess propensity to ventricular arrhythmias, hearts were subjected to four different PES in the absence and presence of 300 nM isoproterenol:

***Frequency-varying burst pacing protocol***– For frequency-varying burst pacing protocol, a set of three trains of stimuli was delivered to the heart. Each train of stimuli consists of 50 stimuli with interval (cycle length) of 100ms and was separated by a pacing-free interval of 2 s. The cycle length is progressively reduced from 100 ms to 20 ms in 10 ms decrements after each set.

***Amplitude-varying burst pacing protocol***– For amplitude-varying burst pacing protocol, a set of three trains of stimuli was delivered to the heart. Each train of stimuli consists of 50 stimuli with interval of 20 ms and was separated by a pacing-free interval of 2 s. The current amplitude was progres-

sively increased by factors of the pacing threshold current, i.e. the minimum current to evoke an action potential in a 1:1 manner). The protocol was terminated when a ventricular arrhythmias was observed or a current of 35 mA was reached.

***Dynamic S1 pacing***– Cycles of a decremental, paced electrogram fractionation sequence comprising a 100-stimulus (S1) drive train were applied at a pacing interval of 135 ms initially. Pacing interval was reduced by 5 ms between successive drive trains until a pacing interval of 10 ms was reached.

***S1S2 pacing***– Cycles of a decremental, paced electrogram fractionation sequence comprising an 8 Hz eight-beat stimulus (S1) drive train, followed by an extra stimulus (S2). Initially, the interval between S1 and S2 was set to be 125 ms and was progressively reduced by 1 ms between successive drive trains until the preparation became refractory.

Ventricular arrhythmia was defined as six or more consecutive regular premature waveforms or irregular fibrillating waveforms. The arrhythmogenicity of the heart was determined by number of protocols that successfully triggered arrhythmias. A scoring system was devised on this basis. For example, the score for arrhythmogenicity is 3 when a heart exhibited signs of arrhythmias under 3 out of 4 protocols. (note: the maximum score was 4 when all four protocols successfully triggered arrhythmias)

#### ***In silico study***

A conformational search in implicit solvent (water) with the OPLS\_2005 force field (60) was performed for SAN4825 using MacroModel Schrödinger Release 2017-1. An adapted blind docking of all possible conformations in the mouse CD38 (PDB ID: 2EG9, chain A) was performed with Glide (61, 62) considering all inside cavities, as determined by SiteMap (63). Protein was prepared using the protein preparation tool available in Maestro, filling in missing side chains and loops with Prime (64, 65) and minimizing the resulting structure with OPLS\_2005 force field. SAN4825's protonation states were predicted by using the Epik software (66). Protein residues' protonation states were determined by PropKa 3.1 (67, 68). Following docking, binding energies were calculated for ranking the best docking conformations using the Molecular Mechanics/Generalized Born Surface Area (MM/GBSA) scoring function. For the scoring, residues close to 5

Å were considered flexible allowing optimization of the docking conformations. To confirm SAN4825 binds only to the active site containing the most important residues for NAADP and cADPR synthesis, SAN4825 was further submitted to a blind docking using the SwissDock server (69, 70). The distance between the predicted binding sites and the active site of CD38 were measured. The center of the active site of CD38 was determined to be the center of geometry of amino acid residues Trp129, Glu150, Asp159, Trp193, Glu230 of mouse CD38. These amino acid residues correspond to Trp125, Glu146, Asp155, Trp189, and Glu226 in human CD38, which are important in CD38-mediated enzymatic syntheses, as identified in a site-directed mutagenesis study (38).

### Drugs and reagents

The SAN4825 compound was a kind gift from Sanofi (Montpellier, France).  $\beta$ -NGD, NADP, NA, nicotineamide, Triton X-100, saponin, and bafilomycin A1 were from Sigma (Saint Louis, MO).

### Statistical analysis

All statistical comparisons were made by two-tailed Student's t-tests unless stated otherwise. Mann-Whitney test and Fisher's exact test were used to compare arrhythmogenicity score and categorical data respectively. As only 1 in 6 hearts from  $CD38^{-/-}$  mice showed arrhythmias, one sample t-test ( $H_0: \mu = 7$ ) was used for statistical analysis in Fig 6E. All data are expressed as mean values  $\pm$  SEM.

**Acknowledgments:** We would like to thank Sanofi for providing the SAN4825 compounds. We would like to thank Dr Daniel Aston for providing rabbit ventricular and atrial myocytes and Dr Grant Churchill for his constructive comments. AG is funded by Wellcome Trust Senior Investigatorship and British Heart Foundation (BHF) Centre of Research Excellence (CRE). RS is funded by BHF and BHF CRE. ML is funded by the BHF, Medical Research Council and BHF CRE.

**Conflict of interest:** The authors declare that they have no conflicts of interest with the contents of this article.

**Author contributions:** WKL carried out all the experiments either solely or in collaborations with ELB (contraction studies), WAC and MJ (docking experiments), YW (MAP recording), FO'B (isolating SR fractions), and MM (sheep cardiac SR experiments). CG provided technical support for plate reader experiments. MR was responsible for the breeding of the  $CD38^{-/-}$  mouse line and JP was the Home Office project license holder. WKL, AG, ML and DAT were responsible for experimental design. All experiments were carried out in the laboratories of DAT, AG, RS and ML. All authors contributed to the writing and editing of the manuscript.



## REFERENCES

1. Ferrero, E., Lo Buono, N., Horenstein, A.L., Funaro, A., and Malavasi, F. (2014) The ADP-ribosyl cyclases—the current evolutionary state of the ARCs. *Front. Biosci. (Landmark Ed)* **19**, 986–1002
2. Howard, M., Grimaldi, J.C., Bazan, J.F., Lund, F.E., Santos-Argumedo, L., Parkhouse, R.M., Walseth, T.F., and Lee, H.C. (1993) Formation and hydrolysis of cyclic ADP-ribose catalyzed by lymphocyte antigen CD38. *Science* **262**, 1056–1059
3. Aarhus, R., Graeff, R.M., Dickey, D.M., Walseth, T.F., and Lee, H.C. (1995) ADP-ribosyl cyclase and CD38 catalyze the synthesis of a calcium-mobilizing metabolite from NADP. *J. Biol. Chem.* **270**, 30327–30333
4. Lee, H.C. (2001) Physiological functions of cyclic ADP-ribose and NAADP as calcium messengers. *Annu. Rev. Pharmacol. Toxicol.* **41**, 317–45
5. Galione, A. (2014) A primer of NAADP-mediated Ca(2+) signalling: From sea urchin eggs to mammalian cells. *Cell calcium* **58**, 27–47
6. Rakovic, S., Galione, A., Ashamu, G.a., Potter, B.V., and Terrar, D.a. (1996) A specific cyclic ADP-ribose antagonist inhibits cardiac excitation-contraction coupling. *Curr. Biol.* **6**, 989–996
7. Macgregor, A., Yamasaki, M., Rakovic, S., Sanders, L., Parkesh, R., Churchill, G.C., Galione, A., and Terrar, D.A. (2007) NAADP controls cross-talk between distinct Ca2+ stores in the heart. *J. Biol. Chem.* **282**, 15302–15311
8. Collins, T.P., Bayliss, R., Churchill, G.C., Galione, A., and Terrar, D.A. (2011) NAADP influences excitation-contraction coupling by releasing calcium from lysosomes in atrial myocytes. *Cell Calcium* **50**, 449–458
9. Capel, R.A., Bolton, E.L., Lin, W.K., Aston, D., Wang, Y., Liu, W., Wang, X., Burton, R.A.B.A.B., Bloor-Young, D., Shade, K.T.T., Ruas, M., Parrington, J., Churchill, G.C., Lei, M., Galione, A., and Terrar, D.A. (2015) Two pore channels (TPC2s) and nicotinic acid adenine dinucleotide phosphate (NAADP) at lysosomal-sarcoplasmic reticular junctions contribute to acute and chronic  $\beta$ -adrenoceptor signaling in the heart. *J. Biol. Chem.* **290**, 30087–30098
10. Rakovic, S. and Terrar, D.A. (2002) Cyclic ADP-Ribose and NAADP. In *Cyclic ADP-Ribose and NAADP*, 319–341. Springer US, Boston, MA
11. Lewis, A.M., Aley, P.K., Roomi, A., Thomas, J.M., Masgrau, R., Garnham, C., Shipman, K., Paramore, C., Bloor-Young, D., Sanders, L.E.L., Terrar, D.A., Galione, A., and Churchill, G.C. (2012)  $\beta$ -Adrenergic receptor signaling increases NAADP and cADPR levels in the heart. *Biochem. Biophys. Res. Commun.* **427**, 326–329
12. Rakovic, S., Cui, Y., Iino, S., Galione, A., Ashamu, G.A., Potter, B.V.L., and Terrar, D.A. (1999) An antagonist of cADP-ribose inhibits arrhythmogenic oscillations of intracellular Ca2+ in heart cells. *J. Biol. Chem.* **274**, 17820–17827
13. Nebel, M., Schwoerer, A.P., Warszta, D., Siebrands, C.C., Limbrock, A.C., Swarbrick, J.M., Fliegert, R., Weber, K., Bruhn, S., Hohenegger, M., Geisler, A., Herich, L., Schlegel, S., Carrier, L., Eschenhagen, T., Potter, B.V.L., Ehmke, H., and Guse, A.H. (2013) Nicotinic acid adenine dinucleotide phosphate (NAADP)-mediated calcium signaling and arrhythmias in the heart evoked by  $\beta$ -adrenergic stimulation. *J. Biol. Chem.* **288**, 16017–16030
14. Kannt, A., Sicka, K., Kroll, K., Kadereit, D., and Gögelein, H. (2012) Selective inhibitors of cardiac ADPR cyclase as novel anti-arrhythmic compounds. *Naunyn Schmiedebergs Arch. Pharmacol.* **385**, 717–27
15. Gul, R., Park, D.R., Shawl, A.I., Im, S.Y., Nam, T.S., Lee, S.H., Ko, J.K., Jang, K.Y., Kim, D., and Kim, U.H. (2016) Nicotinic Acid Adenine Dinucleotide Phosphate (NAADP) and Cyclic ADP-Ribose (cADPR) Mediate Ca2+ Signaling in Cardiac Hypertrophy Induced by  $\beta$ -Adrenergic Stimulation. *PLoS One* **11**, e0149125
16. De Flora, A., Franco, L., Guida, L., Bruzzzone, S., Zocchi, E., and Flora, A.D. (1998) Ectocellular

- CD38-catalyzed synthesis and intracellular  $\text{Ca}^{2+}$ -mobilizing activity of cyclic ADP-ribose. *Cell Biochem. Biophys.* **28**, 45–62
17. Jackson, D.G. and Bell, J.I. (1990) Isolation of a cDNA encoding the human CD38 (T10) molecule, a cell surface glycoprotein with an unusual discontinuous pattern of expression during lymphocyte differentiation. *J. Immunol.* **144**, 2811–2815
18. De Flora, A., Zocchi, E., Guida, L., Franco, L., and Bruzzone, S. (2004) Autocrine and paracrine calcium signaling by the CD38/NAD<sup>+</sup>/cyclic ADP-ribose system. *Ann. N. Y. Acad. Sci.* **1028**, 176–191
19. Bruzzone, S., Guida, L., Sturla, L., Usai, C., Zocchi, E., and De Flora, A. (2012) Subcellular and Intercellular Traffic of NAD<sup>+</sup>, NAD<sup>+</sup> Precursors and NAD<sup>+</sup>-Derived Signal Metabolites and Second Messengers: Old and New Topological Paradoxes. *Messenger* **1**, 34–52
20. Davis, L.C., Morgan, A.J., Ruas, M., Wong, J.L., Graeff, R.M., Poustka, A.J., Lee, H.C., Wessel, G.M., Parrington, J., and Galione, A. (2008)  $\text{Ca}^{2+}$  Signaling Occurs via Second Messenger Release from Intraorganelle Synthesis Sites. *Curr. Biol.* **18**, 1612–1618
21. Zhao, Y.J., Zhang, H.M., Lam, C.M.C., Hao, Q., and Lee, H.C. (2011) Cytosolic CD38 protein forms intact disulfides and is active in elevating intracellular cyclic ADP-ribose. *J. Biol. Chem.* **286**, 22170–22177
22. Zhao, Y.J., Lam, C.M.C., Lee, H.C., and Watson, P. (2012) The membrane-bound enzyme CD38 exists in two opposing orientations. *Science signaling* **5**, ra67
23. Zhao, Y.J., Zhu, W.J., Wang, X.W., Zhang, L.H.H., and Lee, H.C. (2015) Determinants of the membrane orientation of a calcium signaling enzyme CD38. *Biochim. Biophys. Acta.* **1853**, 2095–2103
24. Genazzani, A.A., Empson, R.M., and Galione, A. (1996) Unique inactivation properties of NAADP-sensitive  $\text{Ca}^{2+}$  release. *J. Biol. Chem.* **271**, 11599–11602
25. Graeff, R.M., Walseth, T.F., Fryxell, K., Branton, W.D., and Lee, H.C. (1994) Enzymatic synthesis and characterizations of cyclic GDP-ribose. A procedure for distinguishing enzymes with ADP-ribosyl cyclase activity. *J. Biol. Chem.* **269**, 30260–30267
26. Jamur, M.C. and Oliver, C. (2010) Permeabilization of Cell Membranes. In *Methods in Molecular Biology*, volume 588, 63–66. Humana Press, Totowa, NJ
27. Mahony, L. (1988) Maturation of calcium transport in cardiac sarcoplasmic reticulum. *Pediatr. Res.* **24**, 639–43
28. Michalak, M. (1988) Identification of the  $\text{Ca}^{2+}$ -release activity and ryanodine receptor in sarcoplasmic-reticulum membranes during cardiac myogenesis. *Biochem. J.* **253**, 631–6
29. Sitsapasan, R. and Williams, A.J. (1990) Mechanisms of caffeine activation of single calcium-release channels of sheep cardiac sarcoplasmic reticulum. *J. Physiol.* **423**, 425–439
30. Sitsapasan, R., McGarry, S.J., and Williams, A.J. (1994) Cyclic ADP-ribose competes with ATP for the adenine nucleotide binding site on the cardiac ryanodine receptor  $\text{Ca}^{2+}$ -release channel. *Circ. Res.* **75**
31. Zissimopoulos, S. and Lai, F.A. (2005) Interaction of FKBP12.6 with the cardiac ryanodine receptor C-terminal domain. *J. Biol. Chem.* **280**, 5475–5485
32. Laver, D.R. (2007)  $\text{Ca}^{2+}$  stores regulate ryanodine receptor  $\text{Ca}^{2+}$  release channels via luminal and cytosolic  $\text{Ca}^{2+}$  sites. In *Clin. Exp. Pharmacol. Physiol.*, volume 34, 889–896
33. Sikkil, M.B., Collins, T.P., Rowlands, C., Shah, M., O’Gara, P., Williams, A.J., Harding, S.E., Lyon, A.R., and MacLeod, K.T. (2013) Flecainide reduces  $\text{Ca}^{2+}$  spark and wave frequency via inhibition of the sarcolemmal sodium current. *Circ. Res.* **98**, 286–296
34. Li, L., Mirza, S., Richardson, S.J., Gallant, E.M., Thekkedam, C., Pace, S.M., Zorzato, F., Liu, D., Beard, N.A., and Dulhunty, A.F. (2015) A new cytoplasmic interaction between junctin and ryanodine receptor  $\text{Ca}^{2+}$  release channels. *J. Cell. Sci.* **128**, 951–963

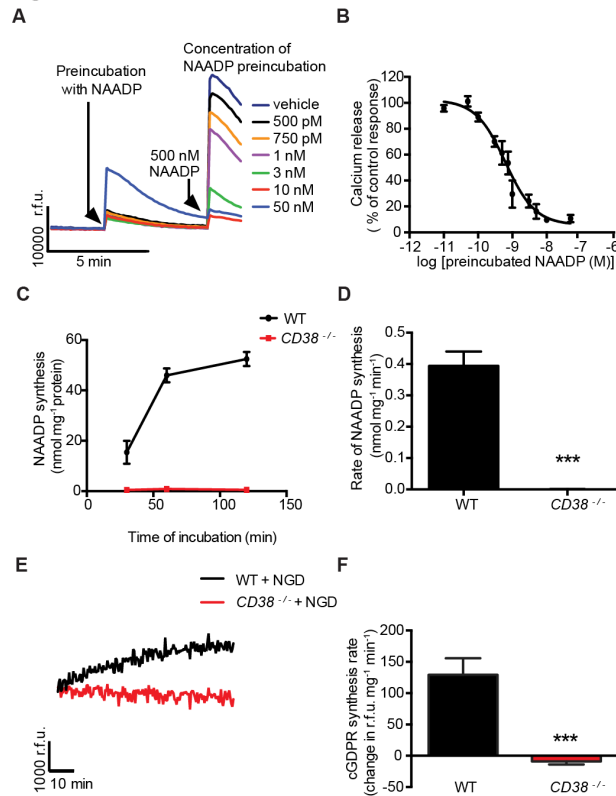
35. Chini, E.N. (2009) CD38 as a regulator of cellular NAD: a novel potential pharmacological target for metabolic conditions. *Curr. Pharm. Des.* **15**, 57–63
36. Aston, D., Capel, R.A., Ford, K.L., Christian, H.C., Mirams, G.R., Rog-Zielinska, E.A., Kohl, P., Galione, A., Burton, R.A.B., and Terrar, D.A. (2017) High resolution structural evidence suggests the Sarcoplasmic Reticulum forms microdomains with Acidic Stores (lysosomes) in the heart. *Sci. Rep.* **7**, 40620
37. Wachter, S.B. and Gilbert, E.M. (2012) Beta-adrenergic receptors, from their discovery and characterization through their manipulation to beneficial clinical application. *Cardiology* **122**, 104–12
38. Munshi, C., Aarhus, R., Graeff, R., Walseth, T.F., Levitt, D., and Lee, H.C. (2000) Identification of the enzymatic active site of CD38 by site-directed mutagenesis. *J. Biol. Chem.* **275**, 21566–21571
39. Hara-Yokoyama, M., Kukimoto-Niino, M., Terasawa, K., Harumiya, S., Podyma-Inoue, K.A., Hino, N., Sakamoto, K., Itoh, S., Hashii, N., Hiruta, Y., Kawasaki, N., Mishima-Tsumagari, C., Kaitsu, Y., Matsumoto, T., Wakiyama, M., Shirouzu, M., Kasama, T., Takayanagi, H., Utsunomiya-Tate, N., Takatsu, K., Katada, T., Hirabayashi, Y., Yokoyama, S., and Yanagishita, M. (2012) Tetrameric interaction of the ectoenzyme CD38 on the cell surface enables its catalytic and raft-association activities. *Structure* **20**, 1585–95
40. Zhang, H., Graeff, R., Lee, H.C., and Hao, Q. (2013) Crystal Structures of Human CD38 in Complex with NAADP and ADPRP. *Messenger* **2**, 44–53
41. Dorian, P. (2005) Antiarrhythmic Action of  $\beta$ -Blockers: Potential Mechanisms. *J. Cardiovasc. Pharmacol. Ther.* **10**, S15–S22
42. Liu, Q., Graeff, R., Kriksunov, I.A., Lam, C.M.C., Lee, H.C., and Hao, Q. (2008) Conformational closure of the catalytic site of human CD38 induced by calcium. *Biochemistry* **47**, 13966–13973
43. Macgregor, A.T., Rakovic, S., Galione, A., and Terrar, D.A. (2007) Dual effects of cyclic ADP-ribose on sarcoplasmic reticulum  $\text{Ca}^{2+}$  release and storage in cardiac myocytes isolated from guinea-pig and rat ventricle. *Cell Calcium* **41**, 537–546
44. Terrar, D. (2015) The Roles of NAADP, Two Pore Channels and Lysosomes in  $\text{Ca}^{2+}$  Signaling in Cardiac Muscle. *Messenger* **4**, 23–33
45. Mészáros, L.G., Wrenn, R.W., and Váradi, G. (1997) Sarcoplasmic reticulum-associated and protein kinase C-regulated ADP-ribosyl cyclase in cardiac muscle. *Biochem. Biophys. Res. Commun.* **234**, 252–256
46. Xie, G.H.H., Rah, S.Y.Y., Yi, K.S., Han, M.K.K., Chae, S.W.W., Im, M.J.J., and Kim, U.H.H. (2003) Increase of intracellular  $\text{Ca}^{2+}$  during ischemia/reperfusion injury of heart is mediated by cyclic ADP-ribose. *Biochem. Biophys. Res. Commun.* **307**, 713–718
47. Saito, A., Seiler, S., Chu, A., and Fleischer, S. (1984) Preparation and morphology of sarcoplasmic reticulum terminal cisternae from rabbit skeletal muscle. *J. Cell. Biol.* **99**, 875–885
48. Holmberg, S.R.M. and Williams, a.J. (1990) The cardiac sarcoplasmic reticulum calcium-release channel: Modulation of ryanodine binding and single-channel activity. *Biochim. Biophys. Acta* **1022**, 187–193
49. Lee, H.C. (2012) Cyclic ADP-ribose and nicotinic acid adenine dinucleotide phosphate (NAADP) as messengers for calcium mobilization. *J. Biol. Chem.* **287**, 31633–40
50. Liu, Q., Kriksunov, I.A., Graeff, R., Munshi, C., Hon, C.L., and Hao, Q. (2005) Crystal structure of human CD38 extracellular domain. *Structure* **13**, 1331–1339
51. Liu, Q., Kriksunov, I.A., Graeff, R., Munshi, C., Hon, C.L., and Hao, Q. (2006) Structural basis for the mechanistic understanding of human CD38-controlled multiple catalysis. *J. Biol. Chem.* **281**, 32861–32869
52. Higashida, H., Egorova, A., Higashida, C., Zhong, Z.G.G., Yokoyama, S., Noda, M., and Zhang, J.S.S. (1999) Sympathetic potentiation of cyclic ADP-ribose formation in rat cardiac myocytes. *J. Biol. Chem.* **274**, 33348–33354

53. Graeff, R., Liu, Q., Kriksunov, I.A., Hao, Q., and Hon, C.L. (2006) Acidic residues at the active sites of CD38 and ADP-ribosyl cyclase determine nicotinic acid adenine dinucleotide phosphate (NAADP) synthesis and hydrolysis activities. *J. Biol. Chem.* **281**, 28951–28957
54. Cosker, F., Cheviron, N., Yamasaki, M., Menteyne, A., Lund, F.E., Moutin, M.J., Galione, A., and Cancela, J.M. (2010) The ecto-enzyme CD38 is a Nicotinic Acid Adenine Dinucleotide Phosphate (NAADP) synthase that couples receptor activation to Ca<sup>2+</sup> mobilization from lysosomes in pancreatic acinar cells. *J. Biol. Chem.* **285**, 38251–38259
55. Venturi, E., Pitt, S., Galfré, E., and Sitsapesan, R. (2012) From Eggs to Hearts: What Is the Link between Cyclic ADP-Ribose and Ryanodine Receptors? *Cardiovasc. Ther.* **30**, 109–116
56. Cockayne, D.A., Muchamuel, T., Grimaldi, J.C., Muller-Steffner, H., Randall, T.D., Lund, F.E., Murray, R., Schuber, F., and Howard, M.C. (1998) Mice deficient for the ecto-nicotinamide adenine dinucleotide glycohydrolase CD38 exhibit altered humoral immune responses. *Blood* **92**, 1324–33
57. Galfré, E., Pitt, S.J., Venturi, E., Sitsapesan, M., Zaccari, N.R., Tsaneva-Atanasova, K., O'Neill, S., and Sitsapesan, R. (2012) Fkbp12 activates the cardiac ryanodine receptor Ca<sup>2+</sup>-release channel and is antagonised by fkb12.6. *PLoS ONE* **7**
58. Noble, J.E. and Bailey, M.J. (2009) Quantitation of Protein. In *Methods in enzymology*, volume 463, 73–95
59. Clapper, D.L., Walseth, T.F., Dargie, P.J., and Lee, H.C. (1987) Pyridine nucleotide metabolites stimulate calcium release from sea urchin egg microsomes desensitized to inositol trisphosphate. *J. Biol. Chem.* **262**, 9561–9568
60. Jorgensen, W.L., Maxwell, D.S., and Tirado-Rives, J. (1996) Development and testing of the OPLS all-atom force field on conformational energetics and properties of organic liquids. *J. Am. Chem. Soc.* **118**, 11225–11236
61. Friesner, R.A., Banks, J.L., Murphy, R.B., Halgren, T.A., Klicic, J.J., Mainz, D.T., Repasky, M.P., Knoll, E.H., Shelley, M., Perry, J.K., Shaw, D.E., Francis, P., and Shenkin, P.S. (2004) Glide: A New Approach for Rapid, Accurate Docking and Scoring. 1. Method and Assessment of Docking Accuracy. *J. Med. Chem.* **47**, 1739–1749
62. Halgren, T.A., Murphy, R.B., Friesner, R.A., Beard, H.S., Frye, L.L., Pollard, W.T., and Banks, J.L. (2004) Glide: A New Approach for Rapid, Accurate Docking and Scoring. 2. Enrichment Factors in Database Screening. *J. Med. Chem.* **47**, 1750–1759
63. Halgren, T.A. (2009) Identifying and characterizing binding sites and assessing druggability. *J. Chem. Inf. Model.* **49**, 377–389
64. Jacobson, M.P., Friesner, R.A., Xiang, Z., and Honig, B. (2002) On the role of the crystal environment in determining protein side-chain conformations. *J. Mol. Biol.* **320**, 597–608
65. Jacobson, M.P., Pincus, D.L., Rapp, C.S., Day, T.J.F., Honig, B., Shaw, D.E., and Friesner, R.A. (2004) A Hierarchical Approach to All-Atom Protein Loop Prediction. *Proteins* **55**, 351–367
66. Shelley, J.C., Cholleti, A., Frye, L.L., Greenwood, J.R., Timlin, M.R., and Uchimaya, M. (2007) Epik: A software program for pKa prediction and protonation state generation for drug-like molecules. *J. Comput. Aided Mol. Des.* **21**, 681–691
67. Søndergaard, C.R., Olsson, M.H.M., Rostkowski, M., and Jensen, J.H. (2011) Improved treatment of ligands and coupling effects in empirical calculation and rationalization of pK<sub>a</sub> values. *J. Chem. Theory Comput.* **7**, 2284–2295
68. Li, H., Robertson, A.D., and Jensen, J.H. (2005) Very fast empirical and rationalization of protein pK<sub>a</sub> values. *Proteins* **61**, 704–721
69. Grosdidier, A., Zoete, V., and Michielin, O. (2011) SwissDock, a protein-small molecule docking web service based on EADock DSS. *Nucleic Acids Res.* **39**, W270–277
70. Grosdidier, A., Zoete, V., and Michielin, O. (2011) Fast docking using the CHARMM force field with EADock DSS. *J. Comput. Chem.* **32**, 2149–2159

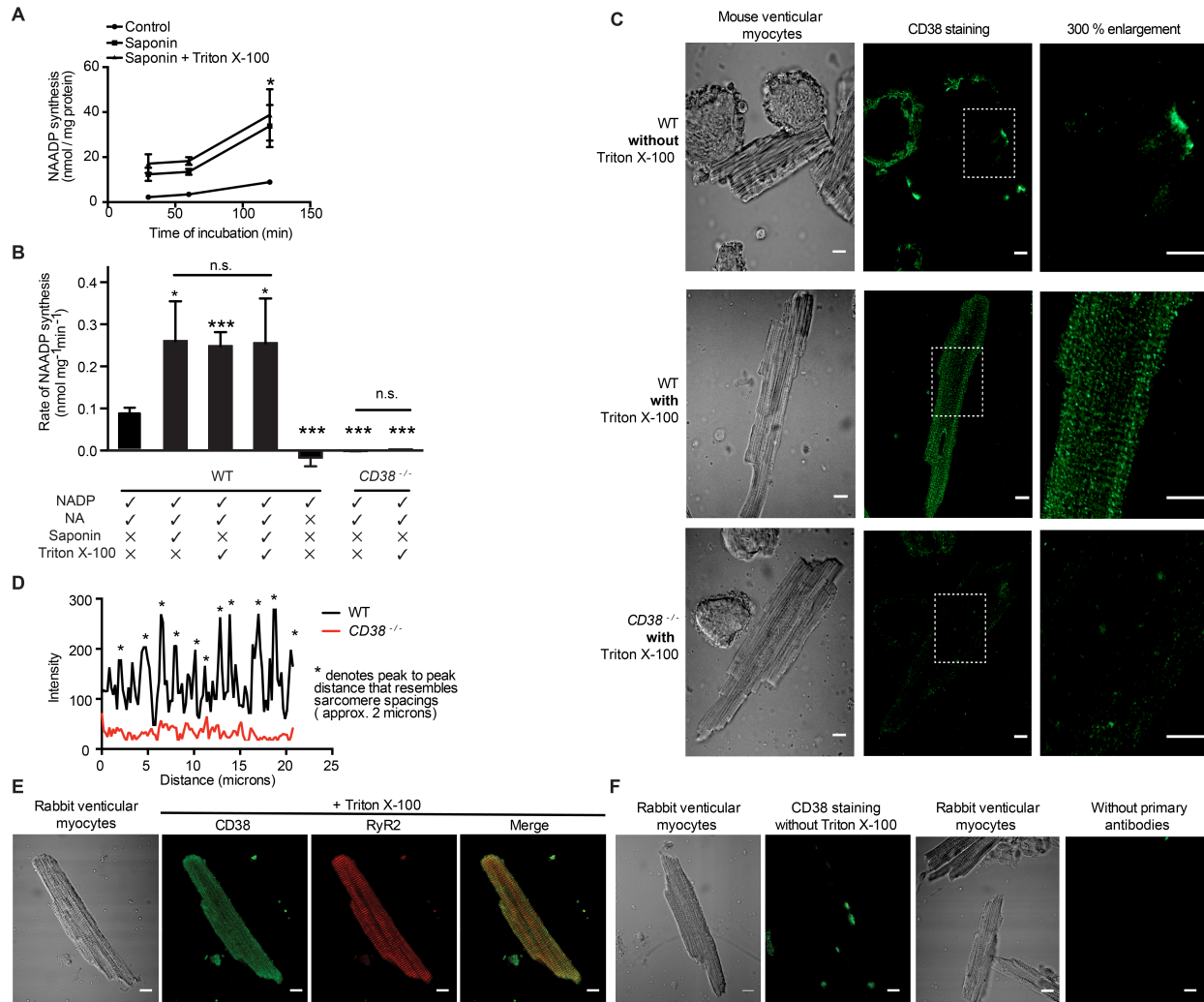


## FIGURES

Figure 1

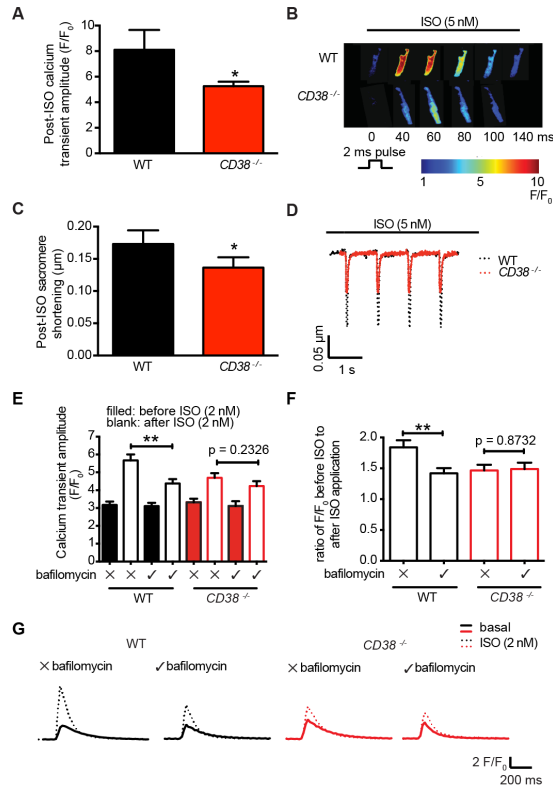


**Figure 1: *In vitro* ADP-ribosyl cyclase activities and NAADP production were not detected in mixed membrane preparation from  $CD38^{-/-}$  mouse heart** Ability of a membrane preparation containing plasmalemma and SR from WT but not  $CD38^{-/-}$  mouse heart to catalyze the synthesis of NAADP and cADPR. **A** shows example traces of the NAADP measurement assay system based on SUEH in which increasing concentrations of NAADP show a desensitization response to the activating substance NAADP. Observations reflecting enhanced desensitization at increasing concentrations of NAADP were used to construct the calibration curve in panel **B**. Using this assay, **C** shows that a membrane preparation WT mice catalysed the synthesis NAADP, while a similar preparation from  $CD38^{-/-}$  mouse heart lacked this ability. The time course of NAADP production is shown in this panel, while **D** shows the average rate of NAADP synthesis from these data ( $n = 4$  for both groups). The membrane preparation from WT mice catalyzed synthesis of cGDPR (an analogue of cADPR) with NGD as a substrate (time course in panel **E**, and bar graph showing the average rate of cGDPR synthesis in panel **F**) while membranes from  $CD38^{-/-}$  mice lacked this ability ( $n = 6$  for both groups). Note that WT membranes showed clear synthesis of both messengers while there was no detectable synthesis with  $CD38^{-/-}$  membranes. Data are expressed as the mean  $\pm$  SEM. \*\*\*  $p \leq 0.001$ ,  $n$  = number of preparations.

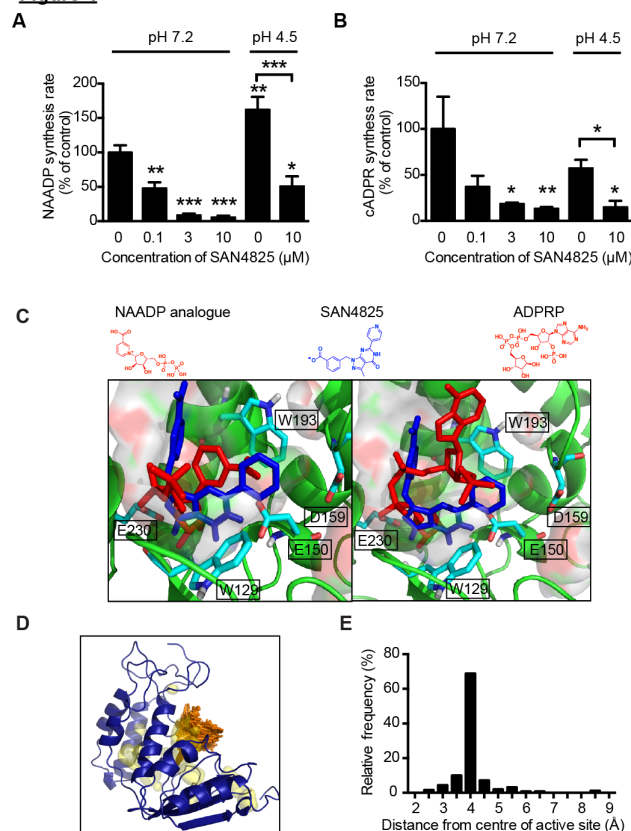


**Figure 2: Permeabilization of cardiac myocytes with Triton X-100 and/or saponin enhanced NAADP production and permitted immunolabeling of CD38.** A shows that the rate of NAADP synthesis was higher after permeabilisation of the cell membranes with saponin alone, and that permeabilisation with TritonX-100 in addition to saponin did not further increase the rate of NAADP synthesis ( $n = 3$  in each group). This point is further illustrated in the bar graph (B), which also shows that the ability to synthesize NAADP was lost in myocytes from  $CD38^{-/-}$  mice ( $n = 4$ ). Omission of NA also abolished synthesis of NAADP in intact cells ( $n = 5$ ). C shows that immunolabeling of CD38 using rabbit anti-human CD38 antibody without Triton X-100 showed little staining, although there were surface patches with higher fluorescence intensity (upper panel). Following membrane permeabilization with Triton X-100 to allow access of the antibody to the cell interior, there was clear staining with a striated pattern in WT (middle panel), but not in permeabilised  $CD38^{-/-}$  cardiac myocytes (lower panel). The representative intensity-distance plot at the bottom of panel D shows that in permeabilized cells the staining observed in the WT myocyte had a much higher intensity than observations in the  $CD38^{-/-}$  myocyte, and showed multiple peaks with a repeating distance interval that resembled the sarcomere spacing. E shows similar observations in rabbit ventricular myocytes. The fluorescent images of myocytes permeabilized with Triton X-100 showed clear labeling with CD38 antibody. There was a striated pattern with a similar spacing to that shown by immunolabeling of RyR2. No labeling with a striated pattern was observed when Triton X-100 or primary antibodies were omitted (F). Images shown are representative staining of the major observation ( $\geq 75\%$ ) in each group ( $n \geq 20$ ). Scale bar = 10  $\mu$ m,  $n$  = number of cells. Data are expressed as the mean  $\pm$  SEM. \*  $p \leq 0.05$ ; \*\*\*  $p \leq 0.001$

Figure 3



**Figure 3: Contribution of NAADP signaling pathway to the  $\beta$ -adrenoceptor-mediated positive inotropy was loss in the  $CD38^{-/-}$  ventricular myocytes  $Ca^{2+}$  transients were triggered by cardiac action potentials in ventricular myocytes from WT and  $CD38^{-/-}$  mice.** The amplitudes of  $Ca^{2+}$  transients in WT (n = 9) and  $CD38^{-/-}$  myocytes (n = 15) are shown in the presence of isoproterenol (A). Example images also shown in B. Under these conditions, amplitudes of CaTs accompanying action potentials were smaller in cardiac myocytes from  $CD38^{-/-}$  mice than WT (B). C shows that sarcomere shortening in the presence of isoproterenol accompanying action potentials was also smaller in myocytes from  $CD38^{-/-}$  mice than WT (WT, n = 12;  $CD38^{-/-}$ , n = 11). Example traces are shown in D. The observations support a functional role for the CD38 enzyme during  $\beta$ -adrenergic receptor stimulation. The effects of isoproterenol on the amplitude of CaTs with and without bafilomycin A1 (10  $\mu$ M) in ventricular myocytes from WT and  $CD38^{-/-}$  mice are shown in E (n = 16-25 in each group). These observations are replotted in F to show the magnitude of the isoproterenol-induced changes with and without bafilomycin A1 in myocytes from WT and  $CD38^{-/-}$  mice. Representative traces are shown in G. Bafilomycin A1 reduced the effect of isoproterenol on the amplitude of CaTs in myocytes from WT but not  $CD38^{-/-}$  mice. The isoproterenol-induced increase in amplitudes of CaTs was therefore less in the presence of bafilomycin A1 in WT myocytes, while in myocytes from  $CD38^{-/-}$  mice the isoproterenol-induced increases in CaT amplitude were similar with and without bafilomycin A1. Data are expressed as the mean  $\pm$  SEM. \*  $p \leq 0.05$ ; \*\*  $p \leq 0.01$ , n = number of cells.

**Figure 4**

**Figure 4: *In vitro* and *in silico* evidence for the action of SAN4825 to inhibit NAADP and cADPR production through targeting CD38.** SAN4825 inhibited NAADP (A) and cADPR (B) synthesis in mouse mixed membrane preparations at both pH 7.2 and pH 4.5. Note that the synthesis of NAADP in the absence of SAN4825 was higher at pH 4.5 than at pH 7.2. C shows the superimposition of the binding conformation of NAADP analogue in human CD38 (left, in red, PDB ID: 4F46, chain B) on the most favorable binding conformation of SAN4825 (left, in blue) in mouse CD38 (PDB ID: 2EG9) at pH 7.2 following Glide docking. A superimposition of binding conformation of ADPRP in human CD38 (right, in red, PDB ID: 4F46, chain A) on the most favorable binding conformation of SAN4825 (right, in blue) in mouse CD38 (PDB ID: 2EG9) is also shown in C (right). D shows the predicted binding sites (orange) for SAN4825 in mouse CD38 following blind docking in SwissDock server. Inner cavities are shown in yellow. The distances between the predicted docking sites and the center of the active site were plotted in a histogram shown in E. Data are expressed as the mean  $\pm$  SEM. \*  $p \leq 0.05$ ; \*\*  $p \leq 0.01$ ; \*\*\*  $p \leq 0.001$ ;  $n \geq 3$  preparations in each group.



Figure 5

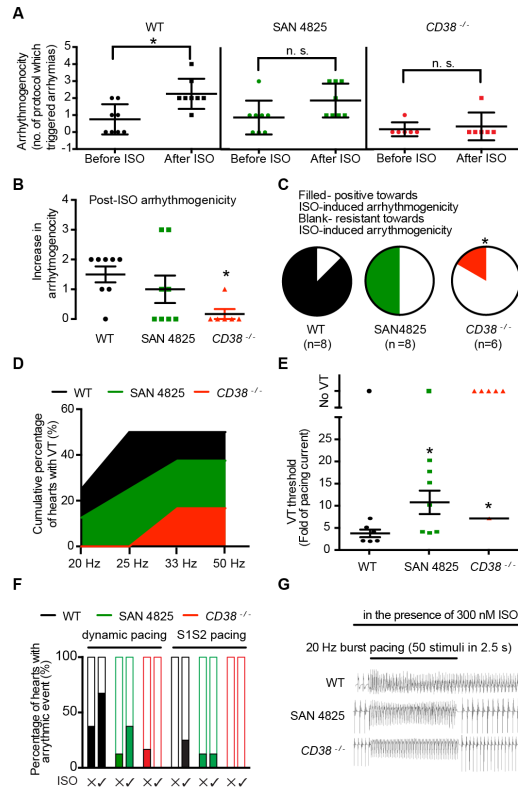


**Figure 5: Hearts from  $CD38^{-/-}$  mice or preincubated with SAN4825 showed resistance to arrhythmias during over-stimulation of  $\beta$ -adrenoceptor pathway** **A** The tendency to show disturbances of rhythm was assessed using four different protocols (see Methods) both before and after exposure to  $\beta$ -adrenoceptor stimulation with isoproterenol (300 nM). In WT hearts, exposure to isoproterenol caused the expected increase in arrhythmias, but this isoproterenol-induced tendency to arrhythmias was suppressed in hearts pretreated with SAN4825 as well as hearts from  $CD38^{-/-}$  mice. **B** (replotted from **A**) shows the increase in arrhythmogenicity of hearts in the presence of isoproterenol. **C** shows the observations in **A** expressed as the proportion of hearts in which isoproterenol increased the tendency to arrhythmias. **D** shows the cumulative percentage of hearts that exhibited arrhythmias in the presence of isoproterenol in the burst pacing experiments with increasing pacing frequency. **E** shows the increase in threshold current required to induce ventricular tachycardia in the presence of isoproterenol. In experiments varying both pacing frequency and current amplitude, hearts from  $CD38^{-/-}$  mice and hearts preincubated with SAN4825 showed reduced tendency to arrhythmias in the presence of isoproterenol. **F** shows the percentages of WT hearts, SAN4825-treated hearts, and  $CD38^{-/-}$  hearts that became arrhythmic (filled bars) during the dynamic pacing and S1S2 pacing experiments, with and without the presence of 300 nM isoproterenol. Representative traces of burst pacing experiments are shown in **G**. Data are expressed as the mean  $\pm$  SEM or percentage. **A** and **B**, Mann Whitney Test; **C**, Fischer exact test; **E**, Student t-test or one-sample t-test \*  $p \leq 0.05$ ; \*\*  $p \leq 0.01$ ; WT,  $n = 8$ ; SAN4825,  $n = 8$ ;  $CD38^{-/-}$ ,  $n = 6$ ,  $n =$  number of hearts.

**Synthesis of the  $\text{Ca}^{2+}$ -mobilizing messengers, NAADP and cADPR, by intracellular CD38 enzyme in mouse heart: role in  $\beta$ -adrenoceptor signaling**

Wee K Lin, Emma L Bolton, Wilian A Cortopassi, Yanwen Wang, Fiona O'Brien, Matylda Maciejewska, Matthew P Jacobson, Clive Garnham, Margarida Ruas, John Parrington, Ming Lei, Rebecca Sitsapesan, Antony Galione and Derek A Terrar

*J. Biol. Chem.* published online May 24, 2017

---

Access the most updated version of this article at doi: [10.1074/jbc.M117.789347](https://doi.org/10.1074/jbc.M117.789347)

Alerts:

- [When this article is cited](#)
- [When a correction for this article is posted](#)

[Click here](#) to choose from all of JBC's e-mail alerts

Supplemental material:

<http://www.jbc.org/content/suppl/2017/05/24/M117.789347.DC1>

This article cites 0 references, 0 of which can be accessed free at

<http://www.jbc.org/content/early/2017/05/24/jbc.M117.789347.full.html#ref-list-1>